



Compact diode laser based light source with alternating dual-wavelength emission at 532 nm

André Müller¹ · Bernd Sumpf¹

Received: 25 February 2020 / Accepted: 29 June 2020 / Published online: 8 July 2020
© The Author(s) 2020

Abstract

Compact nonlinear frequency conversion of a Y-branch distributed Bragg reflector (DBR) diode laser for alternating dual-wavelength laser emission at 532 nm is presented for the very first time. The developed light source, realized on a $5 \times 25 \text{ mm}^2$ micro-optical bench, is based on single-pass second harmonic generation of a 1064 nm Y-branch DBR diode laser in a periodically poled lithium niobate waveguide crystal with superimposed poling periods. Phase-matching is obtained by intrinsic wavelength stabilization of the laser and wavelength tuning by implemented heater elements above the DBR gratings. Obtained optical output powers of 5.6 mW at 532.45 nm and 6.7 mW at 531.85 nm are limited by central lobe power contents of 52% available for waveguide coupling. With a spectral performance showing narrowband emission with spectral widths of 0.01 nm (0.4 cm^{-1}) limited by the spectral resolution of the spectrum analyzer and a spectral spacing of 0.6 nm (20 cm^{-1}), the developed light source is suitable for applications such as Raman spectroscopy and shifted excitation Raman difference spectroscopy (SERDS). Separate electrical contacts of the Y-branch diode laser enable alternating operation at both wavelengths.

1 Introduction

Light sources with an emission wavelength at 532 nm are well-established for numerous applications. At low optical output powers, Raman spectroscopy represents a suitable non-invasive optical measurement technique for specific target analysis at the molecular level. Here, short excitation wavelengths yield larger cross sections and sensitivities with a $1/\lambda^4$ dependence [1]. In addition, emission wavelengths in the visible spectral range can trigger resonance enhancements for some scatterers and, due to the properties of typically used silicon based detectors, are usually measured with higher quantum efficiency and less noise than near-infrared wavelengths. However, these wavelengths also are more likely to excite fluorescence signals masking the Raman signals. Other disturbing signal contributions originate from ambient light when measuring real-world samples under in-situ conditions. Shifted excitation Raman difference spectroscopy (SERDS) has been demonstrated to separate

Raman signals from disturbing background contributions [2]. Subsequent Raman measurements at two slightly shifted excitation wavelengths generate spectrally shifted Raman spectra. Background contributions such as fluorescence and ambient light remain spectrally constant. Subtraction of both spectra therefore efficiently extracts the Raman signals.

Ideal light sources for SERDS on most solid and liquid samples including biological targets should provide narrow bandwidth, alternating dual-wavelength laser emission with a common excitation spot and spectral distances in the range of $\approx 3\text{--}20 \text{ cm}^{-1}$ [3]. In the near-infrared spectral range, compact diode lasers such as distributed feedback (DFB) or DBR lasers fulfill such requirements [4]. Wavelength tuning for alternating dual-wavelength operation suitable for SERDS is obtained by changing the injection current or laser temperature [5]. In order to address narrow bandwidth emission wavelengths in the visible spectral range at around 532 nm, frequency conversion such as second harmonic generation (SHG) in nonlinear crystals can be a method of choice [6]. For SHG, lasers with narrowband laser emission and good spatial beam quality are preferred. Using DFB and DBR lasers, optical output powers $\geq 100 \text{ mW}$ [7, 8] have been generated. A light source at 488 nm suitable for SERDS has been demonstrated by single-pass SHG and a joint

✉ André Müller
andre.mueller@fbh-berlin.de

¹ Ferdinand-Braun-Institut, Leibniz-Institut für
Höchstfrequenztechnik, Gustav-Kirchhoff-Str. 4,
12489 Berlin, Germany

temperature management for the applied 976 nm DFB laser and the nonlinear crystal on a $5 \times 25 \text{ mm}^2$ micro-optical bench [9]. Here, alternating dual-wavelength emission was obtained by changing the heat sink temperature of the device by 8 K and utilizing comparable temperature coefficients of the GaAs based diode laser and the periodically poled lithium niobate waveguide crystal.

As an alternative to tunable single wavelength emission diode lasers, monolithic dual-wavelength Y-branch DBR and DFB diode lasers with output powers up to 200 mW have been presented at 671 nm [10], 785 nm [11] and 976 nm [12]. These lasers consist of two individually controllable laser cavities that are coupled into a common output waveguide using a Y-branch section. Intrinsic gratings for wavelength stabilization in each cavity allow for two laser emission wavelengths with customized spectral spacing. Separate electrical contacts for the two cavities enable alternating dual-wavelength laser emission for SERDS. In addition, implemented heater elements above the individual gratings even allows adjusting the wavelength spacing of the two emission wavelengths for different samples [13].

In this work, compact nonlinear frequency conversion of a Y-branch DBR diode laser for alternating dual-wavelength laser emission at 532 nm suitable for SERDS is presented for the first time. The developed light source is based on single-pass second harmonic generation (SHG) of a 1064 nm Y-branch DBR diode laser in a periodically poled lithium niobate waveguide crystal with superimposed poling periods on a $5 \times 25 \text{ mm}^2$ micro-optical bench. Phase-matching in the nonlinear crystal at both wavelengths is obtained by individual intrinsic wavelength stabilization of the Y-branch laser and wavelength tuning by implemented heater elements above the gratings. First, the optical concept for compact, alternating dual-wavelength single-pass frequency conversion is described. Then, the developed Y-branch DBR diode laser is characterized and corresponding experimental results for SHG including alternating operation at 532 nm are presented.

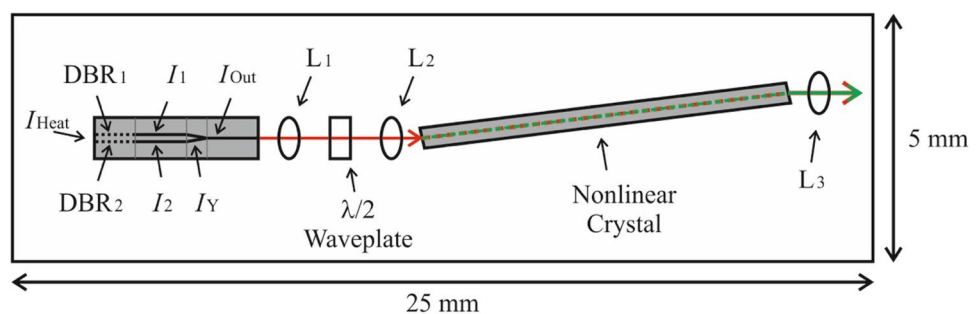
2 Optical concept for compact alternating dual-wavelength SHG

Figure 1 shows the optical concept for compact alternating dual-wavelength SHG with a Y-branch DBR diode laser. The developed diode laser is based on a vertical layer structure established for 1064 nm devices [14]. It consists of an InGaAs triple quantum well, embedded in a $4.8 \mu\text{m}$ asymmetric super large optical cavity. This results in a vertical far field angle of 15° measured at full width at half maximum (FWHM). The 4.0 mm long device has two individually controllable laser cavities, formed between two separate 1.0 mm long tenth order DBR gratings with a lateral pitch of $80 \mu\text{m}$ and a common front facet. Both gratings, DBR_1 and DBR_2 , have grating periods of about $1 \mu\text{m}$ and are designed for emission wavelengths at 1063 nm and 1064 nm, respectively. Numerical simulations indicate that diffraction efficiencies as high as 90% can be obtained with such high order gratings [15]. Implemented resistors as heater elements above the gratings allow wavelength tuning by applying heater currents (I_{Heat}) that result in Joule heating. The two spatially separated ridge waveguides (RW) containing the gratings have a total length of 1.5 mm. They are coupled into a common 0.5 mm output waveguide by a 2.0 mm Y-branch section. The RW width along the device is $4 \mu\text{m}$.

Separate electrical contacts on the p-side of the device as shown in Fig. 1 enable applying individual injection currents to the waveguides (I_1 , I_2), the Y-branch section (I_Y) and the common output (I_{Out}), respectively. Their lengths are 1.35 mm, 0.30 mm, and 1.35 mm, respectively and differ from the underlying waveguide design. Both facets are passivated and anti-reflection (AR) coated with measured rear and front facet reflectivities of 4×10^{-4} and 5%, respectively. The device is mounted p-side up on a CuW heat spreader on a $5 \times 25 \text{ mm}^2$ AlN micro optical bench. This subassembly is mounted on a $25 \times 25 \text{ mm}^2$ conduction cooled package (CCP) mount.

Aspheric lenses, selected based on beam parameters and optical simulations, are used for collimation and coupling the laser emission into the nonlinear waveguide crystal. For collimation a lens (L_1) with a focal length of

Fig. 1 Illustration of the optical concept for compact alternating dual-wavelength single-pass second harmonic generation with a Y-branch DBR diode laser. The diode laser is shown with the separate electric contacts on the p-side of the device that differ in length from the underlying waveguide design (Illustration is not to scale)



$f=1.45$ mm and a numerical aperture of $NA=0.58$ is used. Coupling into the waveguide crystal is obtained with a lens (L_2) with a focal length of $f=2.00$ mm and a numerical aperture of $NA=0.50$. In between both lenses, a half-wave plate is used to tilt the TE-polarization of the diode laser by 90° , required by the waveguide crystal for SHG. All three optical elements are AR-coated for the near-infrared spectral range.

The custom nonlinear crystal is a z-cut periodically poled lithium niobate waveguide crystal with two superimposed poling periods for alternating dual-wavelength SHG (HC Photonics Corp.). The specified target wavelengths are 1064.0 nm and 1065.2 nm at a phase-matching temperature of 35°C . However, due to production tolerances the manufacturer also provided a temperature window of $\pm 10^\circ\text{C}$, in which phase-matching for the individual wavelengths should be obtained. Consequently, the laser emission wavelengths and their wavelength spacing obtained in the green spectral range will depend on the selected crystal temperature. The crystal aperture is $W \times H = 0.5 \text{ mm} \times 1.5 \text{ mm}$, with the waveguide positioned at a height of 1.0 mm. Its dimensions are about $W \times H = 7 \mu\text{m} \times 5 \mu\text{m}$. The crystal length is 9.0 mm. To avoid back reflections into the diode laser, the crystal is AR-coated for the visible and near-infrared spectral range. In addition, its facets have a lateral polishing angle of 6° . Efficient coupling therefore requires tilting the crystal by about 7° with respect to the optical axis. Collimation of laser emission leaving the crystal is obtained with a third lens (L_3), similar to L_2 but AR-coated for the visible spectral range. All optical components including lenses, half-wave plate and nonlinear crystal are mounted onto the micro optical bench using an UV-light curable adhesive.

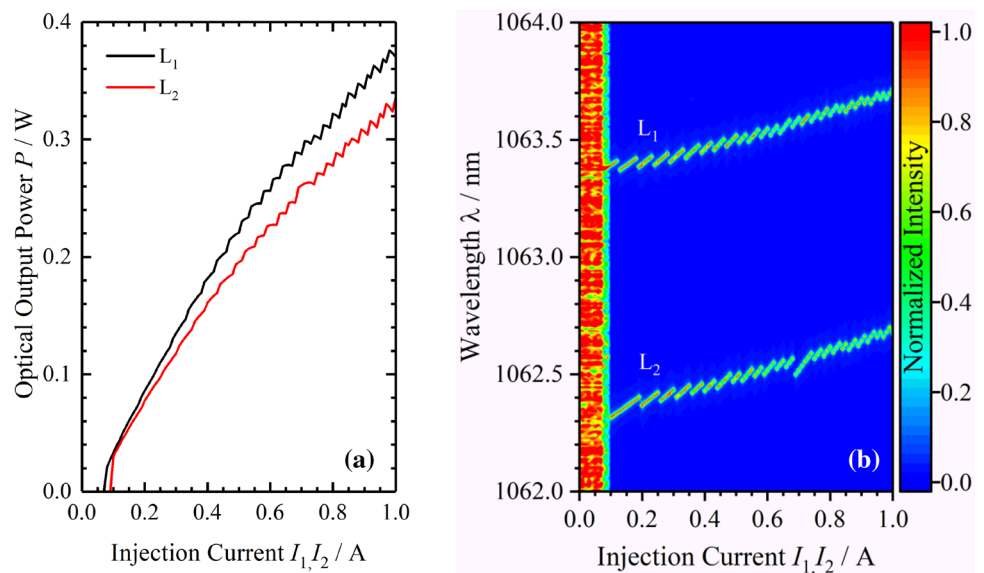
3 Characterization of dual wavelength Y-branch DBR diode laser at 1064 nm

For all measurements, the CCP is mounted on a Peltier-cooled heat sink, stabilized at a temperature of 25°C . The injection current applied to the common output is set to $I_{\text{Out}} = 50$ mA, while no injection current is applied to the Y-branch.

Figure 2a shows the individual power-current characteristics for both branches operated subsequently. The injection currents I_1 and I_2 are increased to 1.0 A in 10 mA steps. In the given example, laser emission starts in the range of 70–90 mA and maximum optical output powers of 0.37 W for laser 1 (L_1) and 0.34 W for laser 2 (L_2) are obtained within the selected injection current range.

Figure 2b shows a false color contour plot of normalized emission spectra obtained for L_1 and L_2 as a function of I_1 and I_2 , respectively. Each spectrum is individually normalized in intensity to 1. The measurement is carried out with a double echelle monochromator (Demon, LTB Lasertechnik Berlin) with a spectral resolution of 14 pm at 1064 nm. At both wavelengths, narrowband laser emission limited by the spectral resolution of the spectrum analyzer is obtained along the whole power range. Mode hops of about 40 pm correspond to the resonator length of 4 mm and are typical for DBR lasers. Laser emission starts at 1063.38 nm for L_1 and 1062.32 nm for L_2 , respectively. At $I_1, I_2 = 1$ A peak emission wavelengths of 1063.71 nm and 1062.68 nm are measured. This corresponds to a temperature related wavelength shift of about 0.4 nm/A. In between mode hops, the measured temperature related wavelength shift is about 1.1 nm/A. At both wavelengths,

Fig. 2 **a** Optical output power of the collimated Y-branch DBR diode laser as a function of I_1 and I_2 . **b** Corresponding normalized emission spectra



spectral widths of about 0.02 nm are measured, limited by the spectral resolution of the spectrum analyzer.

Figure 3a shows a false color contour plot of normalized emission spectra for L_1 and L_2 as a function of I_{Heat} at $I_1, I_2 = 0.5$ A. The heater current is increased to 0.3 A in 10 mA steps. Again, each obtained spectrum is individually normalized in intensity to 1. At $I_{\text{Heat}} = 0.0$ A, emission wavelengths of 1063.44 nm (L_1) and 1062.45 nm (L_2) are measured. Up to $I_{\text{Heat}} = 70$ mA, the temperature related wavelength shifts are within the resolution of the spectrometer. At higher injection currents, both emission wavelengths increase and show a quadratic dependence of the heater current as expected [13]. The peak emission wavelengths at 0.3 A are 1065.22 nm (L_1) and 1064.19 nm (L_2), respectively. This corresponds to a tuning range of about 1.8 nm for both branches within the applied heater current range. Throughout the wavelength tuning, narrowband emission limited by the spectral resolution of the spectrum analyzer is maintained. Figure 3b shows the corresponding optical output power. At $I_{\text{Heat}} = 0.0$ A, optical output powers of 0.22 W (L_1) and 0.20 W (L_2) are measured. Optical output powers of 0.21 W (L_1) and 0.19 W (L_2) at $I_{\text{Heat}} = 0.3$ A indicate a negligible power decrease throughout the wavelength tuning range.

The spatial beam characteristics of a 1064 nm Y-branch DBR diode laser are measured according to the method of the moving slit as described in ISO standard 11146. The normalized intensity distributions in the lateral near field and far field at $P = 0.3$ W are plotted in Fig. 4. Both near field profiles show a defined $4.8 \mu\text{m}$ wide central lobe ($1/e^2$) and distinct side lobes at opposite sides. The side lobe positions can be explained by the waveguide design of the Y-branch laser and are discussed in detail in [16]. Due to the intensity

carried by the side lobes, the resulting central lobe power content is reduced to 52%, available for coupling into the nonlinear waveguide crystal. The obtained far field angles are 13° ($1/e^2$). This results in beam propagation ratios of $M^2 = 3$ ($1/e^2$), taking the side lobes in the near field profiles into account.

4 Experimental results for compact alternating dual-wavelength SHG

For nonlinear frequency conversion, the injection currents to the branches of the diode laser are set to $I_1, I_2 = 1$ A. As shown in Fig. 2a, this results in optical output powers of (0.34–0.37) W. Considering central lobe power contents of 52%, as shown in Fig. 4, the corresponding output power available for SHG in the waveguide crystal is in the range of (0.17–0.19) W. Efficient nonlinear frequency conversion requires phase-matching for the fundamental emission wavelength to the SHG wavelength. In periodically poled crystals, the latter is determined by the poling period and the crystal temperature. Due to a constant heat sink temperature of 25°C selected for the experiments, phase-matching is obtained by wavelength tuning the fundamental emission wavelengths from the Y-branch DBR diode laser using the implemented heater elements. Figure 5a shows the obtained optical output power in the green spectral range as a function of the peak emission wavelengths resulting from wavelength tuning by I_{Heat} . In theory, the intensity obtained by phase-matching as a function of the fundamental wavelength follows a sinc^2 -function. Therefore, the curves for the optical output powers obtained with L_1 and L_2 show multiple distinct maxima. The discrepancy with respect to theoretical

Fig. 3 **a** Normalized emission spectra of the Y-branch DBR diode laser as a function of I_{Heat} at $I_1, I_2 = 0.5$ A. **b** Corresponding optical output power

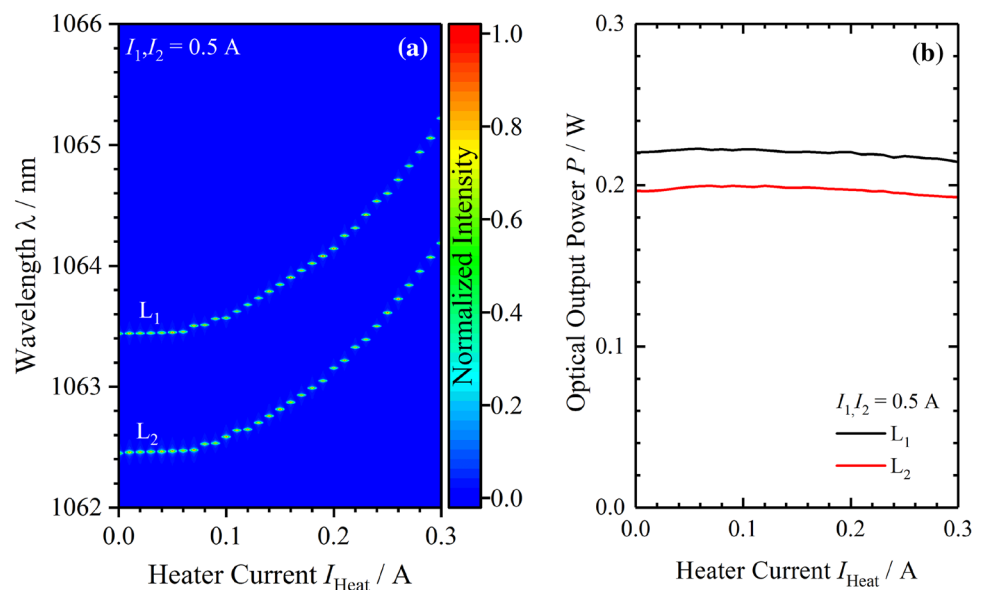


Fig. 4 Normalized intensity distributions of the lateral near field (a) and far field (b) measured at 0.3 W of optical output power

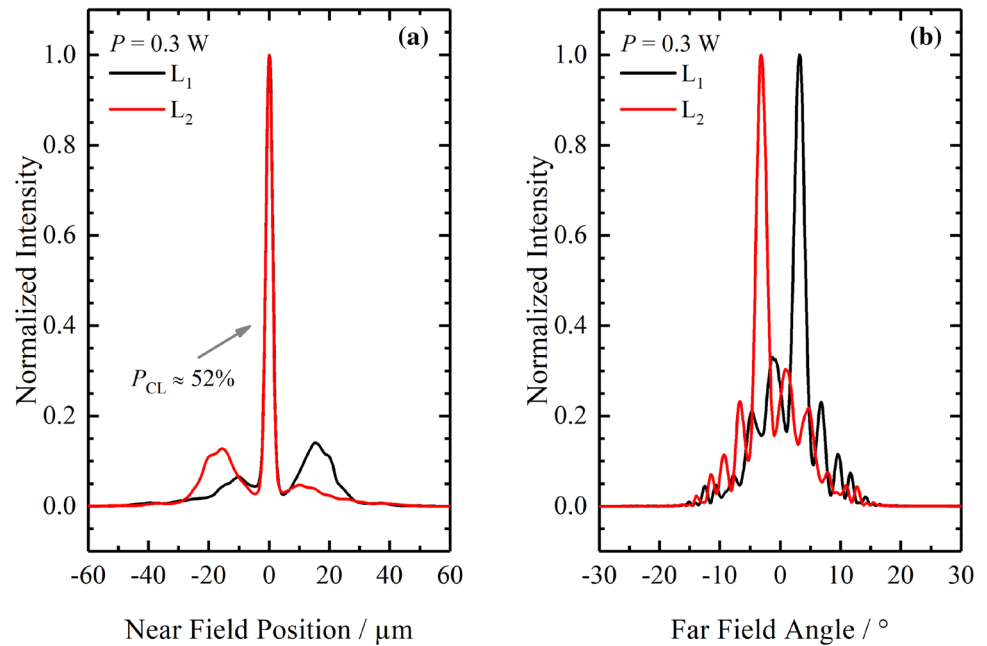
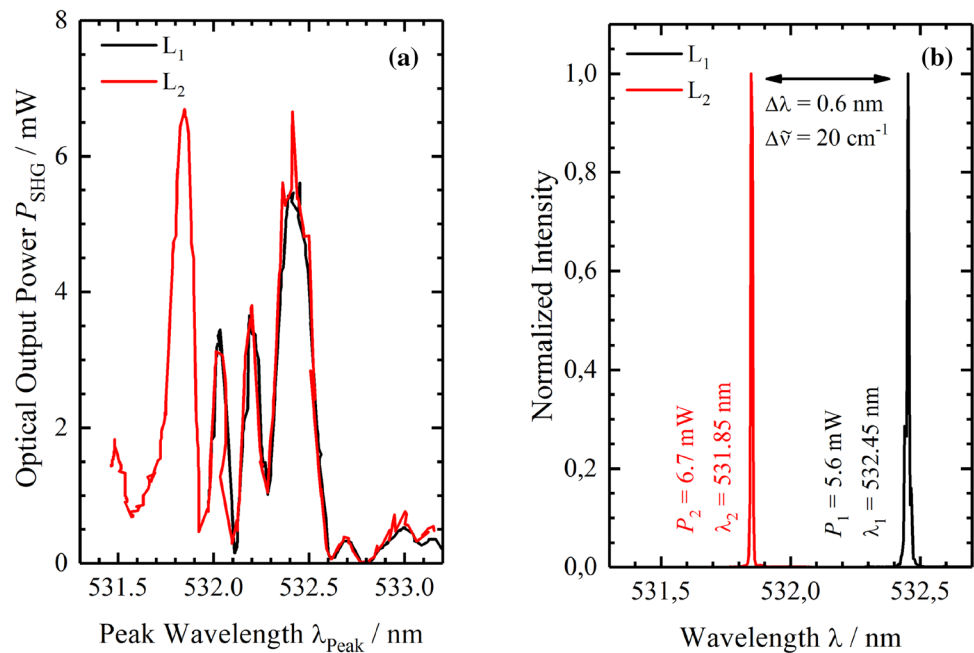


Fig. 5 a Obtained SHG output power as a function of peak emission wavelength resulting from wavelength tuning by I_{Heat} . b Single emission spectra measured at maximum output power



sinc^2 functions is potentially caused by the design of the crystal and the wavelength tuning using the implemented heater elements of the diode laser. At optimum phase-matching, maximum output powers of 5.6 mW (L_1) and 6.7 mW (L_2) are obtained. The measured conversion efficiencies of $\leq 2\%$ with respect to the output power of the Y-branch DBR diode laser can be explained by the above spatial near field intensity distribution of the Y-branch DBR diode laser with central lobe power contents of 52% available for waveguide coupling and the quadratic dependence of the SHG power to the fundamental pump power. Due to the tuning range of

the laser, wavelength tuning for L_2 results in optimum phase-matching at both wavelengths determined by the periodically poled waveguide crystal. As a result, both curves overlap in the wavelength range of 532–533 nm. Figure 5b shows the single emission spectra measured at maximum output power. For both branches, narrowband emission with a spectral width of about 0.01 nm, limited by the spectral resolution of the spectrum analyzer, is obtained. The peak wavelengths are 532.45 nm (L_1) and 531.85 nm (L_2), respectively. This results in a spectral spacing of 0.60 nm (20 cm^{-1}) available for SERDS.

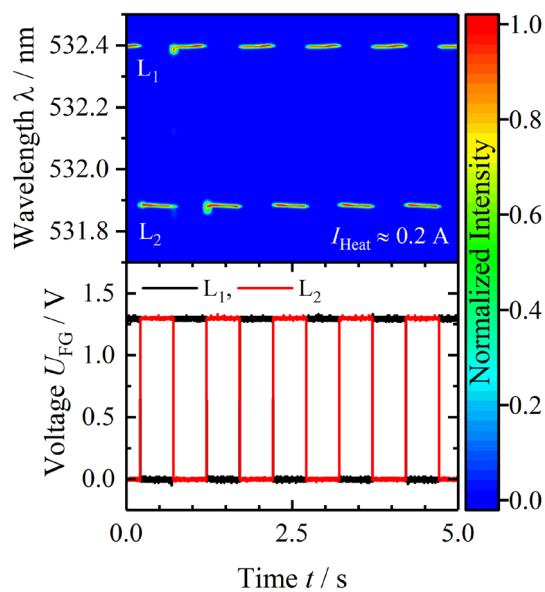


Fig. 6 (Bottom) Modulation signal applied to the injection current of the individual laser branches of the Y-branch DBR diode laser. (Top) Corresponding modulation of the measured laser emission wavelengths

Separate electrical contacts for the individual waveguide sections of the Y-branch DBR diode laser enable an alternating operation of the two branches. Figure 6 shows the measured voltage signals of two frequency generators (U_{FG}) used to modulate the injection current to the branches and the resulting normalized emission spectra. The selected frequency and duty cycle are 1 Hz and 50%, respectively. For both branches, the amplitudes of the square wave signals provided by the frequency generators are set to obtain injection currents of $I_1, I_2 = 1$ A. The selected injection current to the heaters is set to 0.2 A. The plot shows that emission spectra follow the modulation signal. In this example, alternating emission wavelengths of 532.40 nm (L_1) and 531.88 nm (L_2) are obtained. The corresponding spectral spacing of 0.52 nm corresponds to 18 cm^{-1} , available for SERDS. For some pulses, broader spectral widths are observed at the intersection of the applied square wave signals. This might be caused by slight overlaps of the square wave signals and could not completely be removed in this experiment. Throughout the pulses, both emission wavelengths change by ± 4 pm, which is the pixel resolution of the applied spectrum analyzer. However, the apparent increase in case of L_1 and the decrease for L_2 are still under investigation. In addition, instabilities of the second harmonic laser emissions have been observed at higher modulation rates but have not been measured for the Y-DBR laser.

5 Summary

Compact nonlinear frequency conversion of a Y-branch DBR diode laser for alternating dual-wavelength laser emission at 532 nm has been presented for the very first time. The developed light source has been realized on a $5 \times 25\text{ mm}^2$ micro-optical bench. The optical concept is based on single-pass second harmonic generation of a 1064 nm Y-branch DBR diode laser in a custom periodically poled lithium niobate waveguide crystal with superimposed poling periods. Phase-matching at both wavelengths was obtained by individual intrinsic wavelength stabilization of the two laser branches and implemented heater elements above the DBR gratings. The obtained optical output powers of 5.6 mW at 532.45 nm and 6.7 mW at 531.85 nm were limited by the spatial near field intensity distributions with central lobe power contents of 52% available for waveguide coupling. With a spectral performance that showed narrowband emission with spectral widths of 0.01 nm (0.4 cm^{-1}) limited by the spectral resolution of the spectrum analyzer and a spectral spacing of 0.6 nm (20 cm^{-1}), the developed light source is suitable for applications such as Raman spectroscopy and SERDS. Separate electrical contacts for the Y-branch DBR diode laser also enabled alternating operation at both wavelengths.

Acknowledgements Open Access funding provided by Projekt DEAL. The authors acknowledge financial support from the Federal Ministry of Education and Research in the project Exasens under grant number 13N13858 and within the joint program Research Fab Microelectronics Germany.

Open Access This article is licensed under a Creative Commons Attribution 4.0 International License, which permits use, sharing, adaptation, distribution and reproduction in any medium or format, as long as you give appropriate credit to the original author(s) and the source, provide a link to the Creative Commons licence, and indicate if changes were made. The images or other third party material in this article are included in the article's Creative Commons licence, unless indicated otherwise in a credit line to the material. If material is not included in the article's Creative Commons licence and your intended use is not permitted by statutory regulation or exceeds the permitted use, you will need to obtain permission directly from the copyright holder. To view a copy of this licence, visit <http://creativecommons.org/licenses/by/4.0/>.

References

1. R.L. McCreery, *Raman Spectroscopy for Chemical Analysis* (Wiley-Interscience, New York, 2000)
2. A.P. Shreve, N.J. Cherepy, R.A. Mathies, *Appl. Spectrosc.* **46**, 707 (1992)
3. J. Zhao, M.M. Carrabba, F. Allen, *Appl. Spectrosc.* **56**, 834 (2002)
4. G.V. Agrawal, N.K. Dutta, *Semiconductor Lasers*, 2nd edn. (Kluwer Academic Publishers, Dordrecht, 1993)

5. M. Maiwald, G. Erbert, A. Klehr, H.-D. Kronfeldt, H. Schmidt, B. Sumpf, G. Tränkle, *Appl. Phys. B* **85**, 509 (2006)
6. W.P. Risk, T.R. Gosnell, A.V. Nurmikko, *Compact Blue-Green Lasers* (Cambridge University Press, Cambridge, 2003)
7. H.K. Nguyen, M.H. Hu, N. Nishiyama, N.J. Visovsky, Y. Li, K. Song, X. Liu, J. Gollier, L.C. Hughes Jr., R. Bhat, C.-E. Zah, *IEEE Photonics Technol. Lett.* **18**, 682 (2006)
8. Y. Kitaoka, T. Yokoyama, K. Mizuuchi, K. Yamamoto, *Jpn. J. Appl. Phys.* **39**, 3416 (2000)
9. M. Maiwald, H. Schmidt, B. Sumpf, R. Güther, G. Erbert, H.-D. Kronfeldt, G. Tränkle, *Appl. Spectrosc.* **63**, 1283 (2009)
10. M. Maiwald, J. Fricke, A. Ginolas, J. Pohl, B. Sumpf, G. Erbert, G. Tränkle, *Laser Photonics Rev.* **7**, L30 (2013)
11. B. Sumpf, M. Maiwald, A. Müller, J. Fricke, P. Ressel, F. Bugge, G. Erbert, G. Tränkle, *Appl. Phys. B* **120**, 261 (2015)
12. J. Fricke, A. Klehr, O. Brox, W. John, A. Ginolas, P. Ressel, L. Weixelbaum, G. Erbert, *Semicond. Sci. Technol.* **28**, 035009 (2013)
13. B. Sumpf, J. Kabitzke, J. Fricke, P. Ressel, A. Müller, M. Maiwald, G. Tränkle, *Opt. Lett.* **41**, 3694 (2016)
14. K.-H. Hasler, B. Sumpf, P. Adamiec, F. Bugge, J. Fricke, P. Ressel, H. Wenzel, G. Erbert, G. Tränkle, *IEEE Photonics Technol. Lett.* **20**, 1648 (2008)
15. A. Müller, J. Fricke, O. Brox, G. Erbert, B. Sumpf, *Semicond. Sci. Technol.* **31**, 125011 (2016)
16. M. Tawfiq, J. Fricke, A. Müller, P. Della Casa, P. Ressel, A. Ginolas, H. Wenzel, B. Sumpf, G. Tränkle, *Semicond. Sci. Technol.* **33**, 115001 (2018)

Publisher's Note Springer Nature remains neutral with regard to jurisdictional claims in published maps and institutional affiliations.